Currents and Crossroads: Open Quantum System Perspective on Electron Flow and the Mathematical Description of Chemical Selectivity

Grace Hsiao-Han Chuang*[1], Ulf Saalmann[1], Alexander Eisfeld*[1], Josep Maria Bofill[3], Wolfgang Quapp*[2]

hhchuang@pks.mpg.de; eisfeld@mpipks-dresden.mpg.de; quapp@math.uni-leipzig.de

[1]Max Planck Institute for the Physics of Complex Systems, Nöthnitzer Str. 38, D-01187 Dresden, Germany
[2]Mathematisches Institut, Universität Leipzig, Augustus-Platz PF 100920, D-04009, Leipzig, Germany
[3]Química Inorgànica i Orgànica, Secció de Química Orgànica, Universitat de Barcelona, Martí i Franquès 1, 08028 Barcelona, Catalunya, Spain

mpipks Finite Systems

Molecular Aggregate

Definition: Aggregates are **assemblies of monomers** (molecules, atoms, quantum dots, etc.) in which the monomers largely retain their individuality. However, interactions between them can give rise to **collective phenomena** such as superradiance or efficient excitation transfer.
Importance: These collective effects generate **new optical properties**, enabling enhanced light–matter interactions with relevance for optoelectronic and photonic applications.

Distinct Spectral Signature of PTCDA Aggregates on Surface[1]

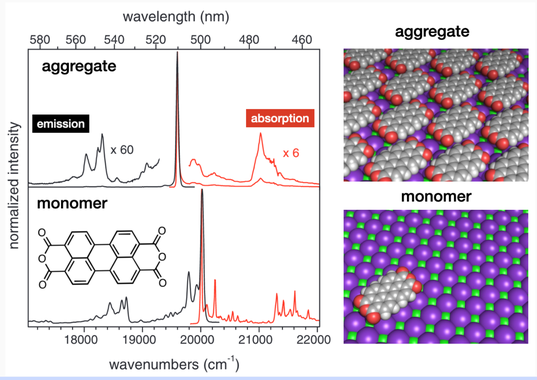

- Shift of 0-0 line
- Strong reduction of vibrational structure
- Relative **enhancement** of 0-0 line: 2.5 times in absorption. and 25 times in fluorescence.

Conventional Hamiltonian in One-Exciton Manifold[2]

The aggregate Hamiltonian is

$$\hat{H}_{\text{agg}} = \sum_{m=1}^{N} \hat{H}_m + \frac{1}{2} \sum_{m=1}^{N} \sum_{\substack{n=1 \\ n\neq m}}^{N} \hat{V}_{mn} \tag{1}$$

$\hat{H}_m$: Hamiltonian for monomer m; $\hat{H}_m = \hat{T}_m^e + \hat{V}_m^{Ne} + \hat{V}_m^{ee}$.
$\hat{V}_{mn}$: Coulomb Interaction between monomer m and n.

Expand Hamiltonian in one-exciton manifold, $|m\rangle = |e\rangle_m \prod_{n\neq m}^{N} |g\rangle_n$, the Frenkel exciton is

$$\hat{H}_{\text{ex}} = \sum_{m=1}^{N} \epsilon_m |m\rangle\langle m| + \sum_{m=1}^{N} \sum_{\substack{n=1 \\ n\neq m}}^{N} V_{mn} |m\rangle\langle n|. \tag{2}$$

The basis for monomer is calculated by solving the electronic time-independent Schrödinger equation (electronic structure theory).

Transition Densities

Transition densities of individual molecules

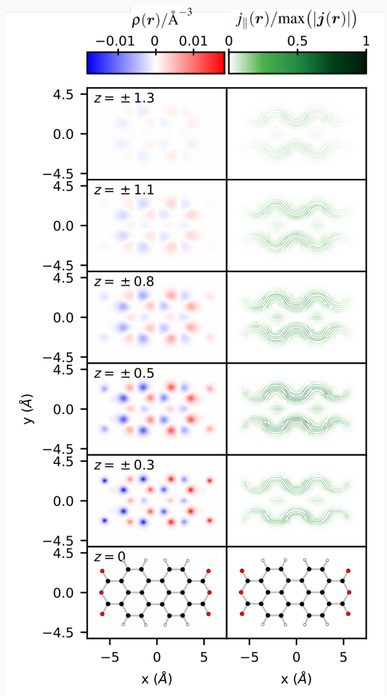

Definitions (relating to figure)
Left: Transition charge density

$$\rho_{ab}(\mathbf{r}) = \langle \phi_a | \sum_k \delta(\mathbf{r} - \mathbf{r}_k) | \phi_b \rangle$$

Right: Transition current density

$$\mathbf{j}_{ab}(\mathbf{r}) = \left\langle \phi_a \middle| \frac{1}{2} \sum_k \Big(\delta(\mathbf{r} - \mathbf{r}_k)\hat{p}_k + \hat{p}_k^\dagger \delta(\mathbf{r} - \mathbf{r}_k) \Big) \middle| \phi_b \right\rangle$$

Definition of transition dipole
From the above quantities, we define transition dipole in different gauges.

1. In length gauge

$$\mu_{ab} = \int \mathbf{r}\, \rho_{ab}(\mathbf{r})\, d^3r$$

2. From velocity gauge

$$d_{ab} = \frac{-i}{\omega_{ab}} \int \mathbf{j}_{ab}(\mathbf{r})\, d^3r$$

3. Global scaling factor

$$s = \frac{|\mu_{ab}|}{|d_{ab}|}$$

Electronic wavefunctions and transition densities are obtained from electronic structure theory. In the grid representation, each quantity is described by roughly one million data points. Calculating **interactions** then requires operations on the full pairwise grid, resulting in on the order of 10^{12} processes!

Coarse-Graining Concepts for Discretisation of Quantities

	$W \approx \sum_{n=1}^{N_A}\sum_{m=1}^{N_B} \frac{q_{ab}^{(A,n)}\, q_{cd}^{(B,m)}}{\lvert \mathbf{r}_n^A - \mathbf{r}_m^B \rvert}$	$V \approx \sum_{n=1}^{N_A}\sum_{m=1}^{N_B} \big(\mathbf{d}_{ab}^{(A,n)}\big)^{\mathsf{T}} \mathbf{T}(\mathbf{r}_n^A, \mathbf{r}_m^B)\, \mathbf{d}_{cd}^{(B,m)}$
$N_A = N_B = 1$	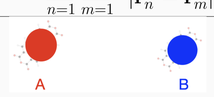	
$N_A \neq 1$ $N_B \neq 1$	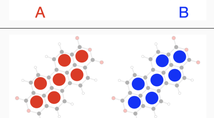	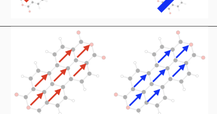

Interaction can be represented through **transition charges (W) or dipoles (V)**. The first row illustrates the point-dipole approximation, which uses a single dipole to represent a molecule. In this project[3], we utilise **multiple** transition charges and dipoles to describe the detailed molecular structure, as shown in the second row.

Numerical Results of Coarse-Graining for PTCDA[3]

# boxes	8	64	512	4096
q	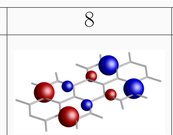	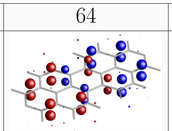	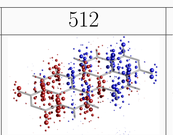	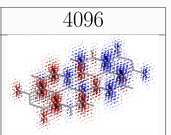
$\mathbf{d}$	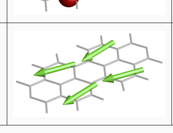	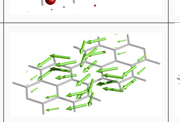	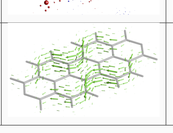	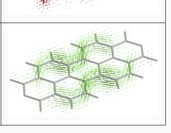

Motivation and Goal

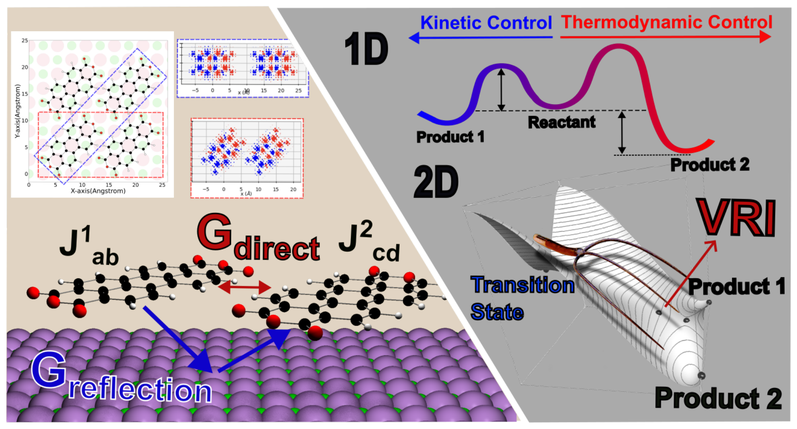

Left: The **interaction** between monomers is modified using a **dyadic Green tensor**, and the **detailed molecular structure** of individual monomers is explicitly captured.
Right: **Selectivity** in asymmetric post-transition-state bifurcation reaction arises from the pitchfork-shaped **local topography** surrounding the valley–ridge inflection point.

Comparison between transition current and charge density

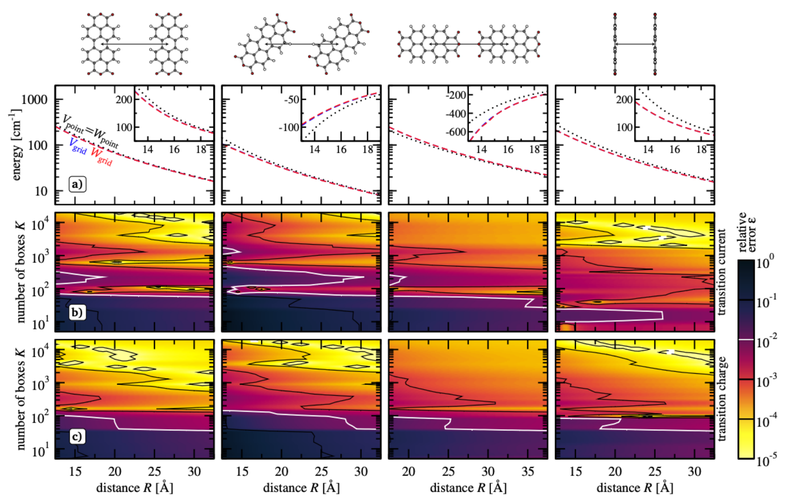

The distance dependence and numerical convergence of interactions for selected molecular arrangements. Panel (a) compares full-grid calculations with point-dipole approximations, showing near-perfect agreement after applying the scaling factor s. Panels (b) and (c) demonstrate convergence with respect to the number of dipoles and point charges, respectively, with relative error contours ($\varepsilon = 1\%$) indicated in white.

Interaction between PTCDA molecules on KCl

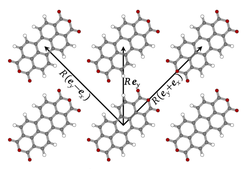

$R = 12.64\text{Å}$, Energy: cm^{-1}

center-to-center	vector	R_{e_y}	$R(e_y + e_x)$	$R(e_y - e_x)$
density (on grid)	W_{grid}	−103.7	−231.6	+92.9
	V_{grid}	−56.0	−128.2	+51.2
	$s^2 V_{\text{grid}}$	−101.4	−232.1	+92.6
point dipoles	W_{point}	−138.6	−196.1	+98.0
	V_{point}	−76.6	−108.3	+54.1
	$s^2 V_{\text{point}}$	−138.6	−196.1	+98.0

The interaction energies of PTCDA dimers adsorbed on KCl for three representative molecular arrangements. The full-grid transition charge and current density calculations agree closely with the point-dipole approximation once corrected by the scaling factor s^2.

Redfield Master Equation

Apply the Coulomb gauge ($\nabla \cdot \hat{\mathbf{A}} = 0$) and the minimum coupling ($\hat{p} \mapsto \hat{p} - q\hat{A}(\hat{\mathbf{r}})$) on Hamiltonian, $\hat{H} = \sum_M \hat{H}_M + \frac{1}{2}\sum_{N\neq M}^{N} \hat{V}_{MN} + \hat{H}_{\text{Field}} + \sum_M \hat{H}_{M,\text{Field}}$. The explicit form of each term is listed below.

$$\hat{H}_M = \sum_{\alpha_M} \frac{\hat{\mathbf{p}}_{\alpha_M}^2}{2m_{\alpha_M}} + \frac{1}{2}\sum_{\alpha_M} \sum_{\substack{\beta_M \\ \beta_M \neq \alpha_M}} \frac{q_{\alpha_M} q_{\beta_M}}{4\pi\epsilon_0 |\hat{\mathbf{r}}_{\alpha_M} - \hat{\mathbf{r}}_{\beta_M}|}$$

$$\hat{V}_{MN} = \frac{1}{2}\sum_{\alpha_M}\sum_{\alpha_N} \frac{q_{\alpha_M} q_{\alpha_N}}{4\pi\epsilon_0 |\hat{\mathbf{r}}_{\alpha_M} - \hat{\mathbf{r}}_{\alpha_N}|}$$

$$\hat{H}_{\text{Field}} = \sum_\ell \int \mathrm{d}^3 r \int_0^\infty d\omega \hbar\omega\, \hat{f}_\ell^\dagger(\mathbf{r},\omega)\hat{f}_\ell(\mathbf{r},\omega)$$

$$\hat{H}_{M,\text{Field}} = \sum_{\alpha_M} q_{\alpha_M}\hat{\varphi}(\hat{\mathbf{r}}_{\alpha_M}) - \frac{q_{\alpha_M}}{m_{\alpha_M}} \hat{\mathbf{p}}_{\alpha_M} \cdot \hat{\mathbf{A}}(\hat{\mathbf{r}}_{\alpha_M})$$

where we define the dummy index as $\alpha_M \equiv \alpha \in M$.

The electric field consists longitudinal and transverse component, where the scaler field ($\hat{\varphi}$) and vector field ($\hat{\mathbf{A}}$) can be related to. And the explicit form of a electric field is

$$\hat{\mathbf{E}}(\mathbf{r},\omega) = \sqrt{\frac{\hbar}{\pi\epsilon_0}\frac{\omega^2}{c^2}} \int \mathrm{d}^3 r' \sqrt{\mathrm{Im}\epsilon(\mathbf{r}',\omega)}\, \boldsymbol{G}(\mathbf{r},\mathbf{r}',\omega)\hat{\mathbf{f}}(\mathbf{r}',\omega),$$

Imϵ is the Imaginary part of the permittivity, $\boldsymbol{G}$ is the classical Green tensor and $\hat{\mathbf{f}}$ is the bonsonic field operator.

In the weak interaction region, we do the second order expansion and then trace out the electric field's degrees of freedom. Under Markov dynamics, the Redfield Master Equation of the reduced density operator is

$$\begin{aligned}\dot{\hat{\rho}}(t) &= \frac{1}{i\hbar}\Big[\sum_M^{N_{\text{Mol}}} \hat{H}_M + \frac{1}{2}\sum_{M\neq N} \hat{V}_{MN}, \hat{\rho}\Big] p + \left(\frac{\partial\hat{\rho}}{\partial t}\right)_{\text{diss}} \\ &= \frac{1}{i\hbar}[\hat{H}_{\text{eff}}\hat{\rho}(t) - \hat{\rho}(t)\hat{H}_{\text{eff}}^+] + f(\text{Quantum fluctuation})\end{aligned}$$

Without the contribution of quantum fluctuation, the resulting effective Hamiltonian is

$$\begin{aligned}\hat{H}_{\text{eff}} &= \sum_n \Big(E_e^m + \sum_{m'\neq m} E_g^{m'}\Big)|\pi_n\rangle\langle\pi_n| \\ &+ \sum_n\sum_m \frac{1}{\epsilon_0 c^2}\int d^3r \int d^3r' \mathbf{j}_{eg}^n(\mathbf{r})\boldsymbol{G}(\mathbf{r},\mathbf{r}',\bar{\omega}_{eg})\mathbf{j}_{ge}^m(\mathbf{r}')|\pi_n\rangle\langle\pi_m|\end{aligned} \tag{3}$$

1. J. Chem. Phys. 139, 044302 (2013).
2. Adv. Energy Mater. 7, 1700236 (2017).
3. J. Chem. Phys. (Submitted Aug. 2025).

Post-Transition-State Bifurcation (PTSB)

Definition: A PTSB occurs when a single transition state bifurcates directly into two products without an intermediate. It represents an intrinsically multidimensional elementary reaction mechanism that requires at least a two-dimensional description (two reaction coordinates) in geometric parameter space.

Selectivity Depends on Potential Energy Surface Topography

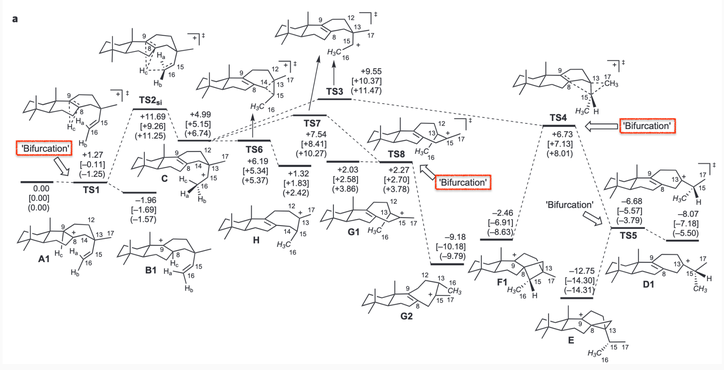

Example of PTSB in biosynthesis[4].

Importance: PTSBs are common in biochemistry and natural product synthesis.
Difficulty: Unlike conventional one-dimensional elementary reaction mechanisms, where selectivity can be rationalised by thermodynamic or kinetic control, PTSBs cannot be explained by these arguments and challenge the foundations of traditional transition-state theory. Most simulations employ Born–Oppenheimer molecular dynamics to **count trajectories** leading to products in order **to predict selectivity**. However, this approach is severely **limited by** (i) the **accessible phase-space volume** and (ii) the **molecular system size**.

Valley–ridge Inflection (VRI) Point

A VRI point is a non-stationary point on the potential energy surface, characterised by a non-zero gradient $\mathbf{g}(\mathbf{x}_{\text{VRI}}) \neq 0$. It satisfies two criteria.

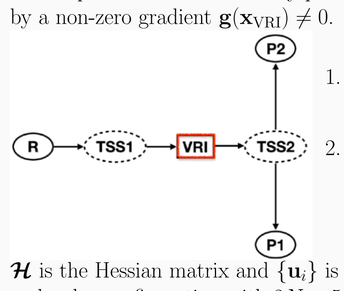

1. The Hessian has one zero eigenvalue,
$$\boldsymbol{\mathcal{H}}_{\text{VRI}}\mathbf{u}_{\text{VRI},i} = 0$$
2. The gradient is orthogonal to the corresponding Hessian eigenvector,
$$\mathbf{g}_{\text{VRI}}^{\mathsf{T}}\mathbf{u}_{\text{VRI},i} = 0$$

$\boldsymbol{\mathcal{H}}$ is the Hessian matrix and $\{\mathbf{u}_i\}$ is the corresponding set of eigenvectors. $\mathbf{x}$ is the molecular configuration with $3N-5$ or $3N-6$ internal degrees of freedom.

Stationary Searching Algorithms

Algorithm	Equation	Initial Conditions
Steepest decent path	$\dot{\mathbf{x}}(s)_{\text{SDP}} = -\frac{\mathbf{g}[\mathbf{x}(s)]}{\lvert\lvert\mathbf{g}[\mathbf{x}(s)]\rvert\rvert}$	TS moves along coordinate
Newton trajectory[5]	$\dot{\mathbf{x}}(s)_{\text{NT}} = \pm\mathbf{A}[\mathbf{x}(s)]\mathbf{g}[\mathbf{x}(s)]$	Select point and initial direction
Gradient extremal	$\boldsymbol{\mathcal{H}}[\mathbf{x}(s)]\mathbf{g}[\mathbf{x}(s)] = \lambda\mathbf{g}[\mathbf{x}(s)]$	
Index boundary	$\det(\boldsymbol{\mathcal{H}}[\mathbf{x}(s)]) = 0$	

The steepest descent path (SDP), also known as the intrinsic reaction coordinate/path (IRC/IRP) in chemistry, cannot bifurcate until a stationary point is reached. $\mathbf{A}$ denotes the adjoint of the Hessian,

$$\mathbf{A} = \frac{\det(\boldsymbol{\mathcal{H}})}{\boldsymbol{\mathcal{H}}}$$

The singular Newton trajectory (NT) satisfies the condition of a VRI, while the gradient extremal provides an alternative approach for locating VRIs.

New Type of VRI: Path without Reactivity[6]

For a general two-dimensional analytical potential energy surface (PES),

$$V(x,y) = x^4 - 2x^2 + y^4 + y^2 - 1.5x^2y^2 + x^2y - cy^3$$

a tunable parameter c modify the PES topography leading to different reactivities.

c	PES
1.5	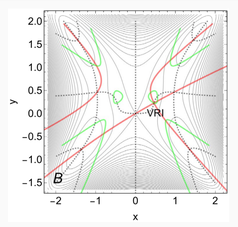
1.125	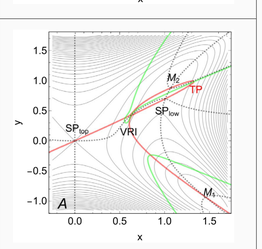
1	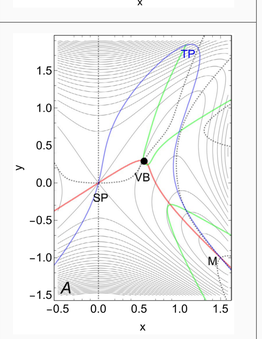

Legend:
standard NT — singular NT
IB — GE

Reactivity regimes:

- **Case c = 1.5 (Standard VRI)**: A standard VRI occurs. The singular NT passes through the VRI, producing the familiar bifurcation of a valley into two distinct pathways.
- **Case c = 1.125 (Intermediate)**: An intermediate situation where stationary points nearly merge into a shoulder. The singular NT persists but becomes distorted, and a turning point (TP) emerges on the index boundary, illustrating the transition between VRI and VB behaviour.
- **Case c = 1 (Dead Valley)**: A new type of valley bifurcation (VB) appears without a ridge in between. The GE crosses the index boundary line, but no singular NT exists. This "dead valley" does not correspond to a reactive bifurcation.

Overall: We identifies a hierarchy of bifurcations: the well-known VRI points, and a weaker form, the VB points, which can exist even without reactivity. Using Newton trajectories (NTs), gradient extremals (GEs), and index boundaries (IBs), the authors show how PES topography can generate both reactive and non-reactive branching patterns.

4. Nat. Chem. 6, 104–111 (2014).
5. Theor. Chem. Acc. 128, 47–61 (2011).
6. Theor. Chem. Acc. 144, 67 (2025).